ISSN 1590-8844
International Journal of Mechanics and Control, Vol. 17, No. 02, 2016

BENCHMARK OF THE ROTORDYNAMICS CAPABILITIES OF THE MOST PROMINENT FINITE ELEMENT METHOD SOFTWARE

Fabio Bruzzone Carlo Rosso

Dipartimento di Ingegneria Meccanica e Aerospaziale - Politecnico di Torino

ABSTRACT

Aim of this paper is to analyze the performance of the most important solvers for finite element method analyses with particular interest to rotordynamics. In order to benchmark their performance in their capability of modelling the effects of gyroscopic moments, the formulation of the gyroscopic damping matrix will be analyzed for both beam and solid elements. Then two reference models will be described for simple rotor geometries that include gyroscopic effects. Then the same rotor geometries will be built in the different software using both beam and solid elements. The obtained Campbell's diagrams will be compared to each other and to the reference models and the conclusions will be drawn.

Keywords: rotordynamics, FEM, software, benchmark, gyroscopic effects

1 INTRODUCTION

With the advent of always increasing computational power availability, more advanced simulation tools have been created that allow to model and simulate the most complex phenomena. One of the hardest dynamic problems to be analytically solved is that of rotors dynamics on which several forces are applied. One of the phenomena that influences more the dynamics of rotating structures is the gyroscopic effect, which causes an apparent stiffening of the body and changes the frequency evolution of the forward and backward whirling modes at the different rotational velocities. Only some of the commercial software for finite element analyses offer the capability to solve this kind of problems but their performance and the correctness of their results appears to have never been compared. Objective of this paper is hence to benchmark the results of four of the main solvers that offer rotordynamic capabilities. Those are namely: MSC Nastran, NX Nastran, Ansys and Samcef. Those software will be tested by comparing the Campbell's diagrams obtained with the models available in literature for two simple rotor geometries that include the effects of gyroscopic moments.

Contact author: Carlo Rosso[1]

[1]Corso Duca degli Abruzzi,24 - 10129 Torino, Italy.
E-mail: carlo.rosso@polito.it

This benchmarking is always performed using a numerical reference, because the goal of the activity is to compare the capabilities of the codes. For a deeper investigation, an experimental campaign has to be used as a reference.

2 SOFTWARE'S ELEMENTS FORMULATIONS FOR THE GYROSCOPIC DAMPING MATRIX

2.1 BEAM ELEMENTS

Suppose that a structure is rotating with rotational velocity $\Omega_X = \dot{\theta}_X$ around the X axis of a Cartesian (OXYZ) inertial reference frame, hence the displacements in the directions perpendicular to the spin axis are u_Y and u_Z. The corresponding rotations are θ_Y and θ_Z and the angular velocities are $\dot{\theta}_Y$ and $\dot{\theta}_Z$. If a precessional velocity is applied to an axis perpendicular to the spin axis, then a reaction moment, called Gyroscopic moment, appears around an axis that is perpendicular to both the spin and precessional velocity axes. For small rotations θ_Y and θ_Z then the instantaneous angular velocity vector is [1]

$$\{\Omega_P\} = \begin{Bmatrix} -\dot{\theta}_Z\theta_Y + \Omega_x \\ \dot{\theta}_Z \sin(\Omega_x t) + \dot{\theta}_Y \cos(\Omega_x t) \\ \dot{\theta}_Z \cos(\Omega_x t) - \dot{\theta}_Z \sin(\Omega_x t) \end{Bmatrix} \quad (1)$$

The kinetic energy of a lumped mass, obtained using (1) is hence

$$E_{Mass}^{Kin} = \frac{1}{2}\begin{Bmatrix}\dot{u}_Y\\ \dot{u}_Z\end{Bmatrix}^T \begin{bmatrix} m & 0\\ 0 & m\end{bmatrix}\begin{Bmatrix}\dot{u}_Y\\ \dot{u}_Z\end{Bmatrix} + \frac{1}{2}\begin{Bmatrix}\dot{\theta}_Y\\ \dot{\theta}_Z\end{Bmatrix}^T \begin{bmatrix} I_d & 0\\ 0 & I_d\end{bmatrix}\begin{Bmatrix}\dot{\theta}_Y\\ \dot{\theta}_Z\end{Bmatrix} - \Omega_X I_p \dot{\theta}_Z \theta_Y \quad (2)$$

where E_{Mass}^{Kin} is its total kinetic energy, m its mass, I_p and I_d are respectively its polar and diametral inertia. The first two terms of (2) contribute to the mass matrix of the elements, while the last to the gyroscopic one. Beam elements are considered as an infinite series of lumped masses, and so the gyroscopic kinetic energy is obtained integrating this term, obtaining

$$E_{Beam}^{Gyro,Kin} = -2\rho\Omega_X I_X \int_0^L \dot{\theta}_Z \theta_Y \, dX \quad (3)$$

where ρ is the material density, I_X is the moment of inertial normal to X and L is the length of the beam element. By using the shape functions [N] for beam elements the gyroscopic damping matrix is obtained. This formulation is shared by all software analyzed.

2.2 SOLID ELEMENTS

The formulation of the gyroscopic damping matrix is instead different among the software and will be dealt separately. MSC Nastran does not have the capability to solve solid rotordynamic analyses and therefore its formulation will not be shown.

2.2.1 NX Nastran

In this software the gyroscopic term is calculated only for the nodes that have rotational degrees of freedom, which is not the case of solid elements. Hence a "surface coat" of shell elements has to be applied on the surface of the solid model. For the nodes created in this way the gyroscopic matrix is calculated as [2]

$$C = \begin{bmatrix} 0 & 0 & 0 & 0 & 0 & 0 & 0 & 0\\ 0 & 0 & 0 & 0 & 0 & 0 & 0 & 0\\ 0 & 0 & 0 & 0 & 0 & 0 & 0 & 0\\ 0 & 0 & 0 & 0 & 0 & 0 & 0 & 0\\ 0 & 0 & 0 & 0 & 0 & \theta_z & 0 & 0\\ 0 & 0 & 0 & 0 & \theta_z & 0 & 0 & 0\\ 0 & 0 & 0 & 0 & 0 & 0 & 0 & 0\\ 0 & 0 & 0 & 0 & 0 & 0 & 0 & 0 \end{bmatrix} \quad (4)$$

where the term θ_z is the Steiner's term of inertia, calculated as

$$\theta_z = \sum m(dx^2 + dy^2) \quad (5)$$

2.2.2 ANSYS and SAMCEF

These two software share the same formulation of the gyroscopic matrix for solid elements, and its derivation is similar to the one for beam elements, and indeed, using the same notation as paragraph 2.1, the kinetic gyroscopic energy is [3] [4] [5]

$$E_{Solid}^{Gyro,Kin} = -\Omega_x \int_{V_i} x(\dot{\theta}_Z y + \dot{\theta}_Y z) dm \quad (6)$$

where in this case V_i is the volume of the ith element. Again, from the kinetic energy, the gyroscopic damping matrix for each element is calculated using the appropriate shape functions [N] for the different kind of solid elements.

3 REFERENCE MODELS

To benchmark the performance of the different software two very well known rotor geometries will be analyzed: the first one is the Stodola/Green rotor, while the second will be the mid-span rotor, often called Jeffcott rotor.

3.1 STODOLA/GREEN ROTOR REFERENCE MODEL

Consider the rotor geometry shown in Figure 1 rotating around the Z axis. The flexible but mass-less shaft has a length S, diameter d and the free end is clamped, so the displacements in any direction, translational or torsional, are denied at this end.

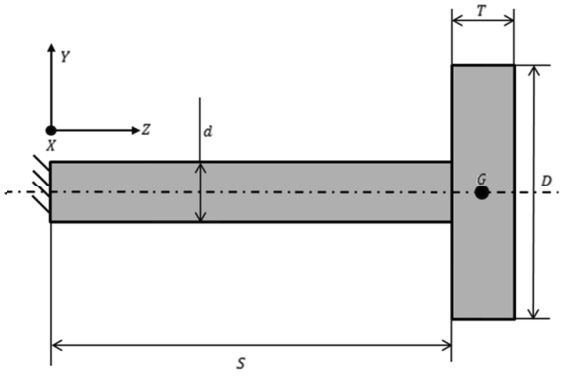

Figure 1 Stodola\Green rotor geometry.

The rigid disk of diameter D, thickness T and total mass m is placed on the other end of the shaft and it is not constrained in any way. The inertia of the shaft and the polar and transverse moments of inertia of the disk can be defined respectively as [6] [7]

$$I = \frac{\pi d^4}{64} \quad (7)$$

$$J_p = \frac{mD^2}{8} \quad (8)$$

$$J_t = \frac{mD^2}{16} \quad (9)$$

The rotor center of mass G will experience the displacements and rotations as depicted in Figure 2, and hence applying Newton's laws and considering that the rotations are small ($\vartheta \approx 0$) the following equations of motion are obtained

$$\begin{cases} m\ddot{x}_G + k_{11}x_G + k_{21}\vartheta_{y,G} = 0 \\ m\ddot{y}_G + k_{11}y_G + k_{12}\vartheta_{x,G} = 0 \\ J_t\ddot{\vartheta}_{x,G} + J_P\Omega\dot{\vartheta}_{y,G} + k_{12}y_G + k_{22}\vartheta_{x,G} = 0 \\ J_t\ddot{\vartheta}_{y,G} - J_P\Omega\dot{\vartheta}_{x,G} + k_{21}x_G + k_{22}\vartheta_{y,G} = 0 \end{cases} \quad (10)$$

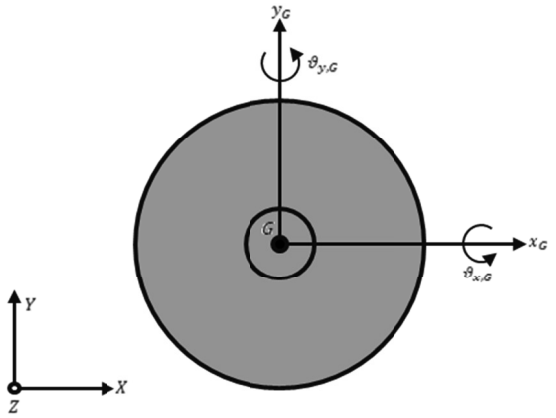

Figure 2 Displacements and rotations experienced by the center of mass G of the disk.

Organizing these equations according to the following vector

$$\{u\} = \begin{Bmatrix} x_G \\ y_G \\ \vartheta_{x,G} \\ \vartheta_{y,G} \end{Bmatrix} \quad (11)$$

and calling $\{\dot{u}\}$ and $\{\ddot{u}\}$ its first and second derivative, the following dynamic system is obtained

$$[M]\{\ddot{u}\} + \Omega[G]\{\dot{u}\} + [K]\{u\} = 0 \quad (12)$$

The stiffness parameters of the shaft are

$$k_{11} = \frac{12EI}{L^3} \quad (13)$$

$$k_{12} = \frac{6EI}{L^2} = -k_{21} \quad (14)$$

$$k_{22} = \frac{4EI}{L} \quad (15)$$

where L is the length of the shaft and E is the Young's modulus of the material. The mass, damping and stiffness matrices obtained are respectively.

$$[M] = \begin{bmatrix} m & 0 & 0 & 0 \\ 0 & m & 0 & 0 \\ 0 & 0 & J_t & 0 \\ 0 & 0 & 0 & J_t \end{bmatrix} \quad (16)$$

$$[\mathrm{G}] = \begin{bmatrix} 0 & 0 & 0 & 0 \\ 0 & 0 & 0 & 0 \\ 0 & 0 & 0 & \mathrm{J_P} \\ 0 & 0 & -\mathrm{J_p} & 0 \end{bmatrix} \quad (17)$$

$$[\mathrm{K}] = \begin{bmatrix} \mathrm{k_{11}} & 0 & 0 & \mathrm{k_{21}} \\ 0 & \mathrm{k_{11}} & \mathrm{k_{12}} & 0 \\ 0 & \mathrm{k_{12}} & \mathrm{k_{22}} & 0 \\ \mathrm{k_{21}} & 0 & 0 & \mathrm{k_{22}} \end{bmatrix} \quad (18)$$

A Matlab code has been developed for computing the results of that model.

3.2 MID-SPAN ROTOR REFERENCE MODEL

Consider now a rotor as shown in Figure 3. The rigid disk of diameter D, thickness T and total mass m is placed at the midpoint of the shaft of total length S and diameter d, so that each portion has length $L = {}^{S}/_{2} - {}^{T}/_{2}$ and both ends are clamped. Proceeding in the same way as in the previous paragraph the same displacement vector (11) and dynamic system (12) are obtained [7] [8], but in this case the matrices are

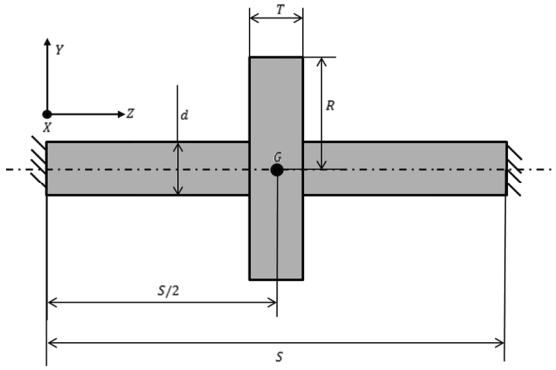

Figure 3 Mid-span rotor geometry.

$$M = \begin{bmatrix} m & 0 & 0 & 0 \\ 0 & m & 0 & 0 \\ 0 & 0 & J_t & 0 \\ 0 & 0 & 0 & J_t \end{bmatrix} \quad (19)$$

$$G = \begin{bmatrix} 0 & 0 & 0 & 0 \\ 0 & 0 & 0 & 0 \\ 0 & 0 & 0 & J_P \\ 0 & 0 & -J_p & 0 \end{bmatrix} \quad (20)$$

$$K = \begin{bmatrix} \alpha & 0 & 0 & 0 \\ 0 & \alpha & 0 & 0 \\ 0 & 0 & \delta & 0 \\ 0 & 0 & 0 & \delta \end{bmatrix} \quad (21)$$

where in this case the inertial properties of the disk are

$$J_p = \frac{mR^2}{2} \quad (22)$$

$$J_t = \frac{m}{4}\left(R^2 + \frac{1}{3}T^2\right) \quad (23)$$

and the stiffness parameters are

$$\alpha = 2 \cdot k \tag{24}$$

$$\delta = k \cdot \left({}^{S}/_{2}\right)^{2} \tag{25}$$

$$k = \frac{48\,EI}{L^3} \tag{26}$$

Solving this system for different rotational velocities Ω the Campbell diagram for the cylindrical (bending) and 1D modes will be plotted, but to obtain more precise results a more accurate approach will also be used for this model. The rotor geometry has been discretized using 61 nodes, forming 60 beam elements according to Timoshenko's beam theory. Each node has four degrees of freedom organized as [9]

$$u_{Node} = \begin{Bmatrix} x \\ y \\ \vartheta_x \\ \vartheta_y \end{Bmatrix} \tag{27}$$

so that for each element the displacement vector is

$$u_{Element} = \{x_1\ x_2\ y_1\ y_2\ \vartheta_{x1}\ \vartheta_{x2}\ \vartheta_{y1}\ \vartheta_{y2}\}^T \tag{28}$$

where the subscripts 1 and 2 indicate the first and second node of each element. The mass matrix is defined as the sum of the translational and rotational contributions so that

$$[M] = [M_t] + [M_r] \tag{29}$$

where

$$M_t = \frac{\rho AL}{420(1+\varphi)^2} \cdot \begin{bmatrix} m_1 & 0 & 0 & m_2 & m_3 & 0 & 0 & -m_4 \\ & m_1 & m_2 & 0 & 0 & m_3 & -m_4 & 0 \\ & & m_5 & 0 & 0 & m_4 & -m_6 & 0 \\ & & & m_5 & m_4 & 0 & 0 & -m_6 \\ & & & & m_1 & 0 & 0 & -m_2 \\ & & & & & m_1 & -m_2 & 0 \\ & & & & & & m_5 & 0 \\ & & & & & & & m_5 \end{bmatrix} \tag{30}$$

$$M_r = \frac{\rho I}{30L \cdot (1+\varphi)^2} \cdot \begin{bmatrix} m_7 & 0 & 0 & m_8 & -m_7 & 0 & 0 & m_8 \\ & m_7 & m_8 & 0 & 0 & -m_7 & m_8 & 0 \\ & & m_9 & 0 & 0 & -m_8 & -m_{10} & 0 \\ & & & m_9 & -m_8 & 0 & 0 & -m_{10} \\ & & & & m_7 & 0 & 0 & -m_8 \\ & & & & & m_7 & -m_8 & 0 \\ & & & & & & m_9 & 0 \\ & & & & & & & m_9 \end{bmatrix} \tag{31}$$

The stiffness matrix is

$$K = \frac{EI}{L^3(1+\varphi)} \cdot \tag{32}$$

$$\cdot \begin{bmatrix} k_1 & 0 & 0 & k_2 & -k_1 & 0 & 0 & k_1 \\ & k_1 & k_2 & 0 & 0 & -k_1 & k_2 & 0 \\ & & k_3 & 0 & 0 & -k_2 & k_4 & 0 \\ & & & k_3 & -k_2 & 0 & 0 & k_4 \\ & & & & k_1 & 0 & 0 & -k_2 \\ & & & & & k_1 & -k_2 & 0 \\ & & & & & & k_3 & 0 \\ & & & & & & & k_3 \end{bmatrix}$$

and the gyroscopic one is simply

$$[G] = 2[M_r] \tag{33}$$

All the coefficients employed in those matrices are listed in Appendix A. As it is evident those matrices are symmetric, especially the gyroscopic one which is instead usually skew-symmetric. Indeed the dynamic system has to be assembled before the solution can proceed, obtaining the following system

$$\begin{bmatrix} [M] & [0] \\ [0] & [M] \end{bmatrix} \{\ddot{u}\} + \Omega \begin{bmatrix} [0] & [G] \\ -[G] & [0] \end{bmatrix} \{\dot{u}\} + \begin{bmatrix} [K] & [0] \\ [0] & [K] \end{bmatrix} \{u\} = \{0\} \tag{34}$$

To model the shaft's clamped ends, the rows and columns corresponding to the first and last nodes of the rotor are deleted: this simulates the eliminations of the degrees of freedom of those two nodes, because with a clamped constraint no displacement or rotation is possible.

3.3 IMPLEMENTATION OF THE REFERENCE MODELS

In order to obtain accurate results, all the previous matrices are used in a tailored Matlab code and considering a high number of degree of freedom. The final problem dimension for the mid-span rotor problem is 472x472. For the same reasons, this approach has also been applied to the Stodola/Green rotor discretizing the geometry using 53 nodes forming 52 beam elements. The final problem dimension is 424x424.

4 BEAM MODELS AND SOFTWARE'S RESULTS

In this paragraph the results obtained from the software for the two rotor cases will be compared. The geometrical, material and FEM model properties are the same for each program and are listed in Table 1 for the Stodola/Green rotor and in Table 2 for the mid-span rotor. The same steel properties will be used throughout this paper and hence will be shown only once. The obtained Campbell's diagrams are compared in Figure 4 and 5 respectively for the Stodola/Green and mid-span rotor with those obtained from the models shown in paragraph 3.1 and 3.2.

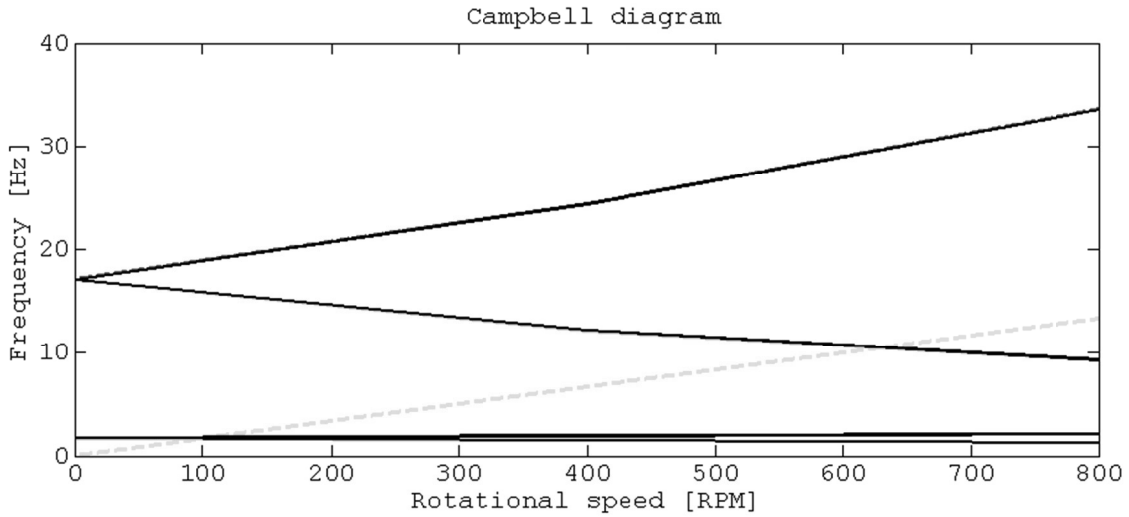

Figure 4 Stodola\Green beam rotor models Campbell's diagrams comparison.

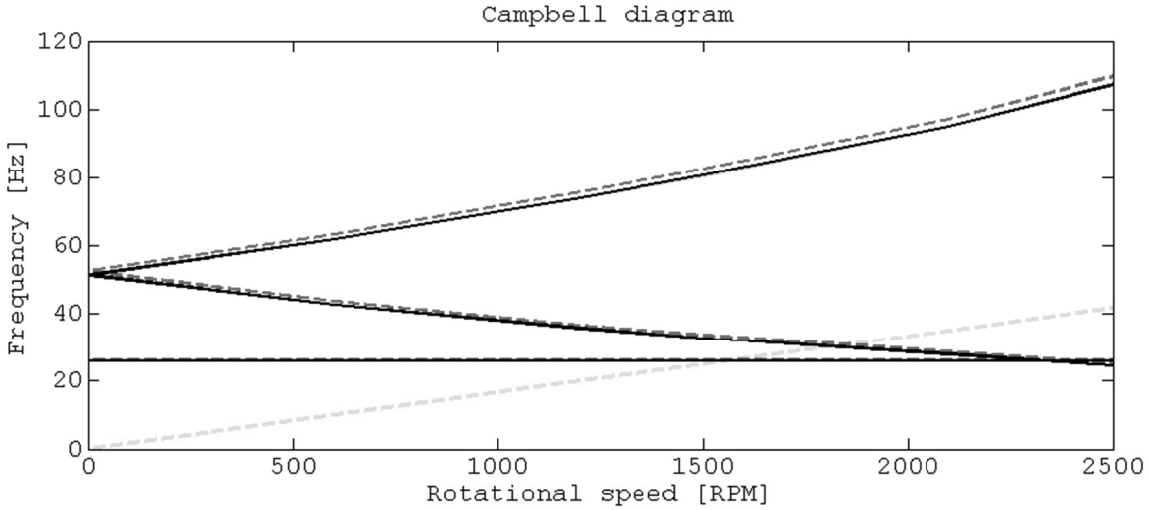

Figure 5 Mid-span beam rotor models Campbell's diagrams comparison.

Table 1: Stodola\Green beam rotor properties

FEM Beam Model	
N° of Nodes	53
N° of Elements	52
Constraint	Clamped end
Ω Range	0÷800 RPM
Material (Steel)	
E	210 GPa
ν	0.3
ρ	7850 kg/m3
Geometrical Properties	
Shaft Diameter	0.05 m
Shaft Length	1.2 m
Disk Diameter	0.6 m
Disk Thickness	0.05 m

Table 2: Mid-span beam rotor properties

FEM Beam Model	
N° of Nodes	61
N° of Elements	60
Constraints	Clamped ends
Ω Range	0÷2500 RPM
Geometrical Properties	
Shaft Diameter	0.04 m
Shaft Length (each)	0.58
Disk Diameter	0.7 m
Disk Thickness	0.04 m

The red dashed lines in those figures represents the results obtained from reference models, the solid black lines are the results from Ansys, the blue ones the results from Samcef, while the green ones are the results from NX Nastran. The cyan dashed line indicates the condition $\Omega = \omega$. The results from MSC Nastran are not shown in those plots because this software only outputs the natural frequencies for the different modes and the rotor energies, but not the evolution of the frequencies at the different rotational speeds.
In the following Table 3 and Table 4, the average relative errors for the bending and 1D modes for the Stodola/Green rotor and for the cylindrical and 1D modes for the mid-span rotor are respectively listed. The average relative error has been calculated as

$$\bar{e} = \frac{\sum_{i=1}^{N} \left(\frac{SOFTWARE_i}{ANALYTICAL_i} - 1 \right) \cdot 100}{N} \tag{35}$$

where N is the number of rotational speeds for which the problem has been solved and i=1,...,N. For MSC Nastran, since the only available frequency is that at 0 RPM the relative error is calculated only for $i = 1$.

Table 3: Stodola\Green beam rotor average relative errors

Bending mode	
MSC Nastran	1.86%
NX Nastran	1.88%
Samcef	1.81%
Ansys	1.81%
1D mode	
MSC Nastran	2.35%
NX Nastran	2.45%
Samcef	2.33%
Ansys	2.31%

Table 4: Mid-span beam rotor average relative errors

Cylindrical mode	
MSC Nastran	1.71%
NX Nastran	2.69%
Samcef	1.18%
Ansys	1.33%
1D mode	
MSC Nastran	1.48%
NX Nastran	1.97%
Samcef	1.08%
Ansys	1.07%

5 SOLID MODELS AND SOFTWARE'S RESULTS

The same geometrical and material properties listed in Table 1 and Table 2 have been used for the solid models for both rotors. 10 nodes tetrahedral solid elements with a mesh size of 2mm has been used in each software for both models, generating 19727 and 21085 elements for the Stodola/Green and mid-span rotor respectively. MSC Nastran has been excluded from this comparison since it is not capable of solving 3D problems [10]. In NX Nastran an additional surface coat of 6 nodes triangular shell elements has been applied for the reasons stated in paragraph 2.2.1. The comparisons of the Campbell's diagrams obtained are shown in Figure 6 and Figure 7 while the average relative errors, calculated again with (35) can be seen in Table 5 and Table 6. The same line colours of Figures 4 and 5 are applied here. The obtained mode shapes from Ansys for the various modes here analyzed can be seen in Figure 8 and Figure 9. As it is evident the errors are larger than for the beam models, which is expected, because the lumped parameters model and the beam formulations are only approximations of the real behavior of the rotors. In the solid models indeed the flexibility of the disks is taken into account. Regarding NX Nastran it is now evident that the approximation in the formulation apparently has negative effects on the prediction of the gyroscopic moment influence, because the evolution of the frequencies as the rotational velocity increases are completely different from the values obtained by the 1D beam model.

Table 5:Stodola\Green solid rotor average relative errors

Bending mode	
NX Nastran	7.82%
Samcef	2.34%
Ansys	2.34%
1D mode	
NX Nastran	47.35%
Samcef	3.71%
Ansys	3.22%

Table 6: Mid-span solid rotor average relative errors

Cylindrical mode	
NX Nastran	4.06%
Samcef	1.86%
Ansys	1.93%
1D mode	
NX Nastran	58.26%
Samcef	4.03%
Ansys	3.59%

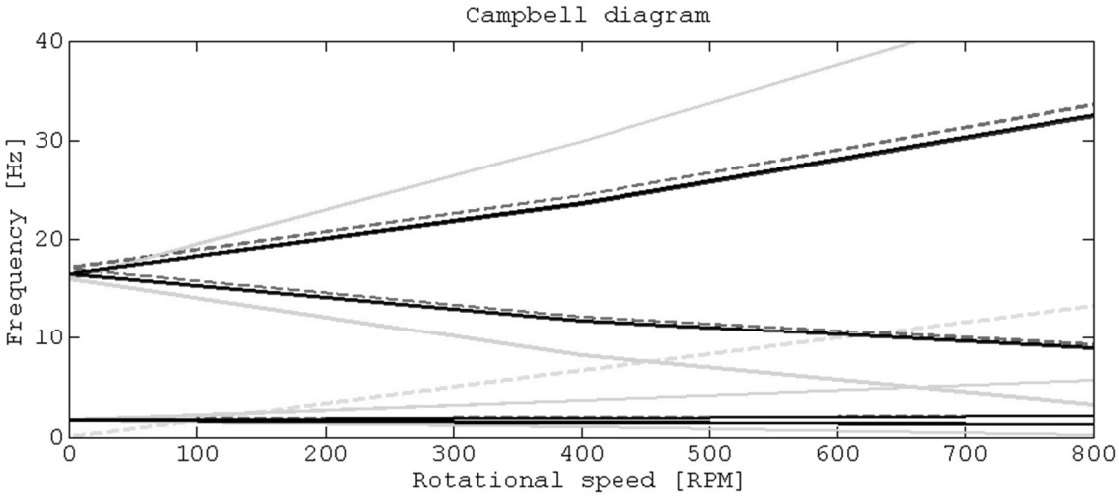

Figure 6 Stodola\Green solid rotor models Campbell's diagrams comparison.

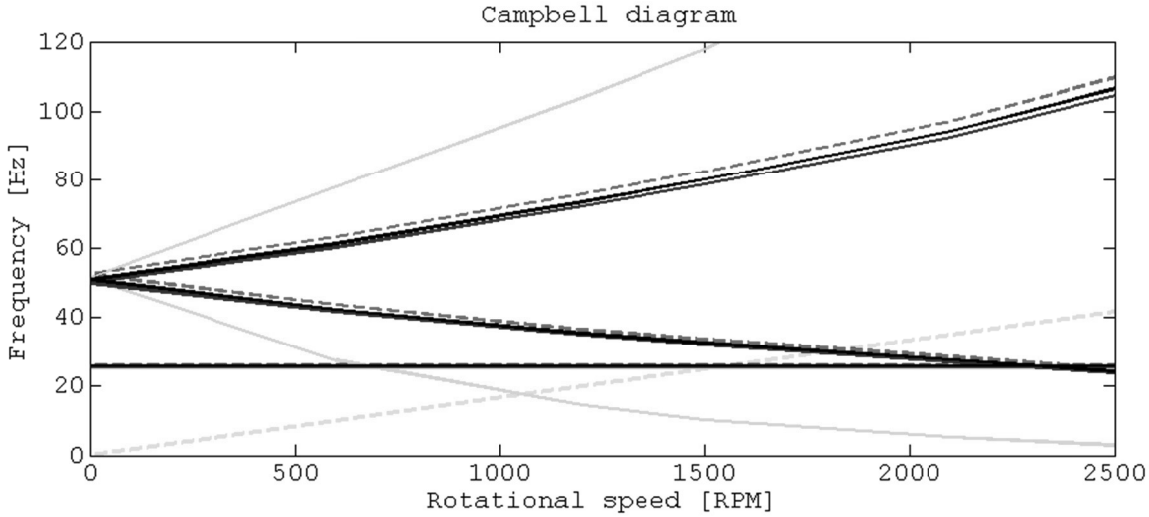

Figure 7 Mid-span solid rotor models Campbell's diagrams comparison.

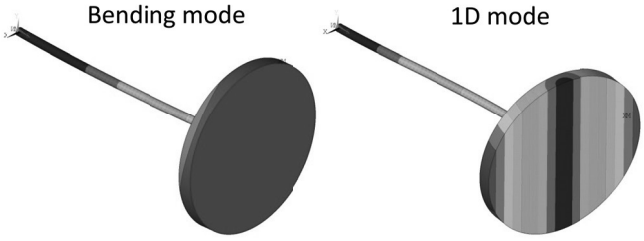

Figure 8 Stodola\Green solid rotor mode shapes obtained from Ansys.

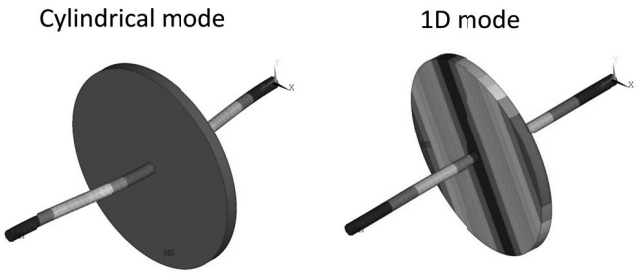

Figure 9 Mid-span solid rotor mode shapes obtained from Ansys.

6 BENCHMARK CONCLUSIONS

Now that the results for all the different beam and solid models from the different software have been compared, it is possible to draw the conclusions. MSC Nastran is not capable of performing any kind of 3D solid rotor dynamic analysis and also the results for this kind of analysis are not complete and clear even for beam models. NX Nastran in theory has those capabilities, but evidently only the beam elements formulation is complete, while the one for solid elements seems to be very approximated, since the results show large discrepancies with the 1D beam model predictions. There is not a real gyroscopic moments formulation, but the software considers only the additional inertia of the shell elements placed on the surface of the model. The results for the beam models are comparable with the other software, but not at all for the solid ones. The last two remaining software, Samcef and Ansys, yield almost the same results in any of the model described before and those are very close to the equivalent 1D beam model, which is widely used and generally accepted as correct. Although both could be hence used in this kind of analyses, Ansys presents an additional feature with respect to Samcef. This is mainly because in Samcef Field many parameters, elements attributes and other aspects of the model are decided by the software and if the user wants to modify some of those values then the text input file to the solver modules are to be modified. This is a difficult task and it is time consuming also because the documentation is not so clear. In Ansys instead the user has the ability to control every aspect of the model if using the Mechanical APDL language. Using this approach it is also possible to setup one "solution script" and use it, with minimal and quick changes, to study very different models, and still be sure of obtaining correct results.

ACKNOWLEDGMENTS

The authors would like to thank the GreatLab facility of GE Avio Aero, born in partnership with Politecnico di Torino, where the analyses in this paper have been performed.

REFERENCES

[1] H.D. Nelson, J.M. McVaugh, The dynamics of rotor-bearing systems using finite elements, *ASME Journal of Manufacturing science and Engineering*, May 1976.
[2] *Siemens PLM NX Nastran User manual.*
[3] M. Geradin, N. Kill, A new approach to Finite Element modelling of flexible rotors, *Engineering Computing*, Vol. 1, 1984.
[4] *Ansys Mechanical APDL User manual.*
[5] *Siemens PLM Samcef User manual.*
[6] D. W. Childs, *Turbomachinery Rotordynamics: Phenomena, Modelling and Analysis*, Wiley&Sons, New York, 1993.
[7] G. Genta, *Dynamics of rotating systems*, Springer, Torino, 2004.
[8] S.Y. Yoon, Z. Lin, P.E. Allaire, *Control of surge in centrifugal compressors by active magnetic bearings*, Springer, New York, 2013.
[9] S. Jones, *Finite elements for the analysis of rotor-dynamic systems that include gyroscopic effects*, Brunel University, 2005.
[10] *MSC Nastran User manual.*

APPENDIX A

The coefficients used in the matrices (30), (31), (32) and (33) are defined as follows:

$$m_1 = 156 + 294\varphi + 140\varphi^2$$
$$m_2 = L(22 + 38.5\varphi + 17.5\varphi^2)$$
$$m_3 = 54 + 126\varphi + 70\varphi^2$$
$$m_4 = L(13 + 31.5\varphi + 17.5\varphi^2)$$
$$m_5 = L^2(4 + 7\varphi + 3.5\varphi^2)$$
$$m_6 = L^2(3 + 7\varphi + 3.5\varphi^2)$$
$$m_7 = 36$$
$$m_8 = L(3 - 15\varphi)$$
$$m_9 = L^2(4 + 5\varphi + 10\varphi^2)$$
$$m_{10} = L^2(1 + 5\varphi - 5\varphi^2)$$
$$k_1 = 12$$
$$k_2 = 6L$$
$$k_3 = L^2(4 + \varphi)$$
$$k_4 = L^2(2 - \varphi)$$

with

$$A = \pi r^2$$
$$\chi = \frac{7 + 6\nu}{6(1 + \nu)}$$
$$\varphi = \frac{12EI\chi}{GAL^2}$$